






Harnessing CNN for Early Breast Cancer Detection: Enhancing Precision in Image-Based Diagnosis



Weny Amelia¹, Salisa 'Asyarina Ramadhani^{2*}, Budi Sunaryo^{3,4}, Ria Desnita¹, Nur Fadjri Nilakesuma⁵

¹ Nursing Science Study Program, Department of Health and Science, Universitas Mercubaktijaya, Padang 25146, Indonesia

² Electrical Engineering Study Program, Faculty of Science and Technology, Universitas Jambi, Jambi 36361, Indonesia

³ Computer Network Engineering Technology, Faculty of Industrial Technology, Universitas Bung Hatta, Padang 25142, Indonesia

⁴ Department of Electrical Engineering, Faculty of Engineering, Universitas Andalas, Padang 25163, Indonesia

⁵ Midwifery Education Study Program, Department of Health and Science, Universitas Mercubaktijaya, Padang 25146, Indonesia

Corresponding Author Email: salisaar@gmail.com

Copyright: ©2025 The authors. This article is published by IETA and is licensed under the CC BY 4.0 license (<http://creativecommons.org/licenses/by/4.0/>).

<https://doi.org/10.18280/isi.300219>

ABSTRACT

Received: 10 December 2024

Revised: 16 January 2025

Accepted: 14 February 2025

Available online: 27 February 2025

Keywords:

mobile phone imaging, image preprocessing, automated segmentation, deep learning

Breast cancer is a critical health problem that needs early detection to ensure better treatment outcomes, especially in rural or underserved areas where mammography access is limited. The following study introduces a new method that allows patients to stay home, capture breast images with a smartphone, and receive real-time detection results via a web application without traveling to urban centers. It aims to bring early detection closer by leveraging deep learning, specifically CNNs. The dataset consisted of 138 images of the breast taken from smartphones, both cancerous and non-cancerous cases, 80% of which were used for training and the remaining 20% for testing. All images were preprocessed to ensure the quality of the data. The CNN model yielded an accuracy of 81%, proving the effectiveness of deep learning in detecting breast cancer. Integrating an easy web application enables patients to acquire preliminary information about their health status and seek immediate medical consultation. In summary, ensuring access to advanced diagnostic tools is crucial for fair early screening of breast cancer, particularly in low-resource areas. This approach combines new technologies with a focus on patient needs to lower barriers to early detection and improve health outcomes worldwide.

1. INTRODUCTION

Breast cancer is one of the most common types of cancer worldwide. It is the most commonly diagnosed cancer in women, according to the World Health Organization, with an estimated 2.3 million new cases annually as of the year 2020 [1]. The widespread incidence of this condition poses significant challenges to public health and imposes substantial emotional and financial burdens on patients, families, and healthcare systems collectively.

The rising awareness of breast cancer underscores the significance of early detection and diagnosis [2-4]. Technological advancements, particularly in imaging and artificial intelligence, have created new avenues for enhancing screening methodologies [5, 6]. Standardized detection systems are challenging to create since data capture variability is influenced by geographic location, socioeconomic level, and healthcare access [7-9]. This diversity may lead to inconsistent diagnostic and treatment outcomes, necessitating exploring innovative strategies to bridge these gaps.

In the very exciting area of developing CNN-driven (Convolutional Neural Network) technologies, there is significant promise for breast cancer screening utilizing

smartphone photos [10, 11]. This revolutionary strategy could democratize access to breast cancer tests by combining the ubiquitous use of cell phones with advanced artificial intelligence capabilities. Facilitating prompt and precise evaluations seeks to enhance the accessibility of breast cancer screening, irrespective of personal situations or geographic obstacles.

To further improve the robustness of CNN models in breast cancer detection using smartphone images, the inclusion of techniques that will reduce the effects of data variability is important [12]. Most promising in this regard is the use of data augmentation strategies, which virtually increase the size of the training dataset with transformations like scaling and changes in color [13]. This approach enhances model generalization and rectifies the problems of over-fitting, especially when training with small-sized datasets, as is often the case in resource-constrained settings [14]. Moreover, incorporating transfer learning can benefit from pre-trained networks on more extensive image banks, thus speeding up training and improving classification accuracy, with the possibility of obtaining predictive accuracies of more than 86% [15]. By adopting these methodologies, researchers can create more resilient diagnostic tools capable of delivering

reliable results across diverse imaging conditions, ultimately fostering equitable access to early breast cancer detection for women worldwide.

Several studies have investigated sophisticated methods for detecting breast cancer, building on this basis and producing noteworthy outcomes. The integration of clinical health records and mammography pictures, for example, showed that multimodal data could increase diagnostic accuracy, with an accuracy of 84.5% [16]. CNNs have been used to classify malignant cells in histopathological pictures with 82% accuracy [17], their application to mammography images produced 84% accuracy [18, 19]. Furthermore, innovations in CNN architecture, such as residual connected CNNs, have pushed the limits of performance, obtaining the greatest recorded accuracy of 85.5% in histopathology image categorization.

Although these findings are promising, there are still challenges to overcome. The lack of a standardized testing platform limits the comparison of different approaches. The absence of result deployment in practical applications, such as online or mobile platforms, impedes real-world integration. Addressing these gaps and applying data augmentation and transfer learning can help to bridge the gap between experimental findings and clinical implementation. By extending these efforts, researchers can increase the reliability and accessibility of diagnostic devices, resulting in earlier detection and better outcomes for breast cancer patients

worldwide.

Furthermore, the quality of smartphone images used in breast cancer detection can be improved to a great extent by including user-friendly mobile applications that provide real-time feedback and guidance during image capture [20]. These apps can offer users tips on lighting conditions or angles to normalize the inputted data, reducing variability and improving model training outcomes. Moreover, by including machine learning algorithms in such apps, even tentative analyses can be performed so that users get insight into their imaging read-outs before seeking advice from healthcare providers. This two-pronged solution gives control to the patient regarding his health. Ultimately, such advances may close the gap in the association between technical capabilities and practical accessibility in fostering a global proactive stance towards breast cancer screening.

2. METHODS

This research was carried out in several stages, including data acquisition, image preprocessing, the development of a Convolutional Neural Network (CNN) model, and the evaluation of the model's performance [14, 21, 22]. The entire system flow is illustrated in Figure 1, with each stage explained in detail below.

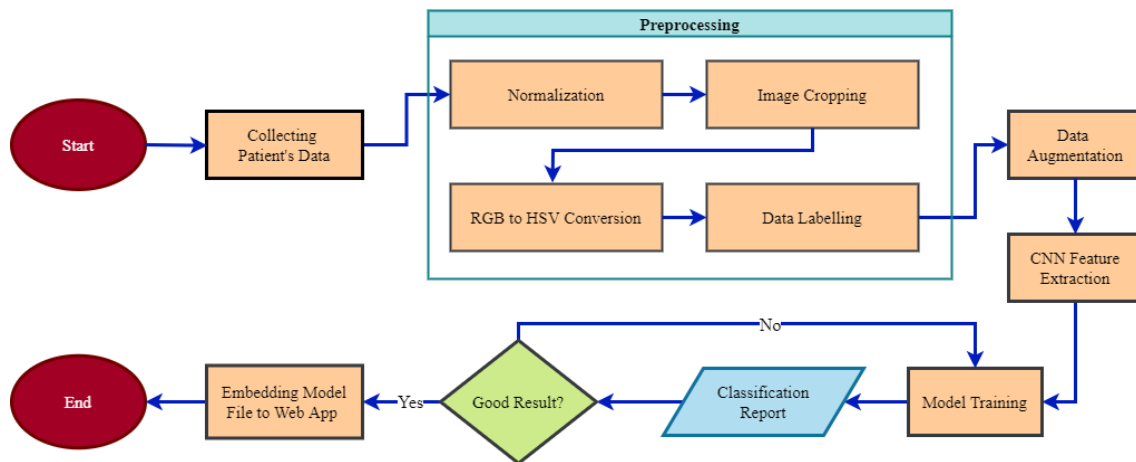


Figure 1. System flowchart

2.1 Data acquisition

The image data used in this study were collected from breast cancer patients who had not undergone mastectomy in West Sumatra. The dataset comprised two categories: photos demonstrating the presence of cancer and images showing no cancer symptoms. These photos were labeled "kanker" and "nonkanker," respectively. A total of 138 photos were acquired, consisting of 69 images of cancer and 69 images of noncancer. The photographs obtained gave a wide representation of breast cancer symptoms, which was necessary for training the CNN to recognize the patterns suggestive of malignancy.

Specific criteria were followed throughout data gathering to ensure uniformity and quality. Images were shot with the patient's smartphone cameras with a minimum resolution of 13 megapixels. HDR (High Dynamic Range) and AI (Artificial Intelligence) features were turned off to avoid

artificial enhancements or alterations. Each photograph portrayed only one breast, captured from a frontal viewpoint with a predetermined distance of 20 cm between the camera and the breast. These parameters assured dataset uniformity [23], giving a solid platform for subsequent processing and analysis.

2.2 Image preprocessing

Data collection was followed by data preparation. The preparation process involves image normalization, which transforms all pixel values to a scale of [0, 1] by dividing each pixel by 255 [24]. The model learned more effectively due to the normalization of the input values. Next, all images were downsized to (150 × 150) pixels to ensure consistency during the training phase, which is critical for convolutional procedures.

The photos were manually cropped to decrease differences

between views, keep key breast regions, and reduce noise. The image was then segmented to separate critical regions of interest (ROI) for targeted analysis, reduced computing costs, and increased feature extraction accuracy [25].

Data augmentation like rotation, flipping, and zooming were utilized to improve the training dataset and lower the likelihood of overfitting. These tactics boosted the diversity of the training data while preventing the model from becoming highly specialized in detecting specific traits within the constrained sample.

2.3 CNN model development and feature extraction

Feature extraction was the starting point in the formulation of the CNN model. Images were first converted from the RGB color space to the HSV color space to represent hue, saturation, and value components—which are much more effective in representing color-based features. Images, after conversion, were segregated into two categories based on their classification: cancerous and non-cancerous. Furthermore, the conversion from RGB to HSV color space ensures that variations in lighting conditions do not significantly impact the output, as the hue and saturation components are less sensitive to brightness changes compared to the RGB representation. This preprocessing step helps to standardize the features extracted from smartphone-captured images under different lighting environments, thereby improving the model's robustness and consistency.

Data augmentation addressed data limitations and improved the model's generalization capability using the ImageDataGenerator function. Later on, the pixel values of the images were scaled within a range from 0 to 1 by dividing each value by 255. A dataset consisting of 138 images must be divided into training and validation subsets. Thus, 80% of the data comprising 112 images was allocated for training, while 20% was reserved for validation, totaling 26 images.

The CNN model itself was constructed with a series of layers utilizing the ReLU activation function on all hidden layers, introducing non-linearity to improve the learning capability of the model. The output layer employed the sigmoid activation function, which is suitable for binary classification. The Adam optimizer was used for efficient weight updates to compile the model, and binary cross-entropy was selected as the loss function, given its effectiveness in handling binary classification problems. The training phase involved running the model for 10 epochs, balancing sufficient learning with preventing overfitting.

2.4 Model evaluation

The model performed with 20% of the overall dataset set aside as validation data. The performance in this validation set tested the model's generalization on new unseen data. Accuracy, precision, recall, and F1-score are several metrics used to describe model performance [26, 27]. Accuracy quantified the overall percentage of right predictions, whilst precision, recall, and F1-score offered more granular information about the model's ability to correctly identify "kanker" cases vs false positives and negatives. The total metrics were examined using macro and weighted averaging. A confusion matrix was also utilized to analyze the prediction distribution, emphasizing correct and incorrect classifications [28]. Training assessment findings were recorded and reviewed to understand the system's overall effectiveness

better and identify areas for improvement. More experiments were conducted to increase the model's performance, such as evaluating different parameter values and investigating architectural improvements. The equations of the metrics can be seen in Eqs. (1)-(6).

$$Accuracy = \frac{TP + TN}{TP + TN + FP + FN} \quad (1)$$

$$Precision = \frac{TP}{TP + FP} \quad (2)$$

$$Recall = \frac{TP}{TP + FN} \quad (3)$$

$$F1 - Score = 2 \times \frac{Precision \times Recall}{Precision + Recall} \quad (4)$$

$$MacroAvg = \frac{1}{C} \sum_{i=1}^C Metric_i \quad (5)$$

$$WeightedAvg = \frac{\sum_{i=1}^C N_i \times Metric_i}{\sum_{i=1}^C N_i} \quad (6)$$

True Positive (TP) is when a model correctly detects a critical item. A False Positive (FP), on the other hand, is when the model thinks an event is essential, but it is not. It is also called a false alarm. A False Negative (FN) is when the model fails to detect a significant event (a missed detection). Lastly, a True Negative (TN) reflects the model's accurate determination that no important event is present [26, 29]. In macro and weighted averaging, the symbol C represents the number of classes, while $Metric_i$ denotes the value of the assessed metric. A higher number of True Positives and True Negatives indicates that the model is more effective.

3. RESULTS AND DISCUSSION

3.1 Result

The development process of this study's CNN-based breast cancer detection model includes 10 main steps in Algorithm 1. The first step is loading the cancer and non-cancer image datasets, followed by the second step of converting the image colors from RGB to HSV to improve the quality of visual analysis. The third step involves clustering the images based on the labels "kanker" and "nonkanker." The fourth step is data augmentation to increase the variety of the training dataset. After that, in the fifth step, a CNN model is built using an architecture specifically designed for image pattern recognition. The model is trained in the sixth step with the processed dataset, and in the seventh step, the model's performance is evaluated using the test dataset. The trained model is then saved in pickle file format in the eighth step. Furthermore, in the ninth step, the model is integrated into a web-based application for real-time prediction. Finally, the tenth step is testing the web-based application to ensure its ability to provide accurate image predictions.

All 138 images in the dataset were preprocessed from RGB to HSV color format. This conversion improved color contrast between cancerous and non-cancerous tissue for easier visual and algorithmic interpretation. The output of this color transformation contains more visual patterns, which helps the second step of training work. For example, color conversion

results on the dataset are outlined in Figure 2: Figure 2(a) shows the conversion results for the image "kanker", and Figure 2(b) shows the image "nonkanker" conversion results. These are representations of a 9-pixel chunk of the dataset, selected to show the color attributes of each category. According to the analysis, cancer images have less saturation and more brightness, whereas non-cancer pictures have more saturation but less brightness. Such patterns are essential for separating image classes in the second analysis stage.

Algorithm 1: Breast Cancer Classification Algorithm
Step 1: Load the breast cancer and noncancer dataset
Step 2: Normalization and image cropping
Step 3: Color extraction (convert from RGB to HSV)
Step 4: Separating images based on "Kanker" and "Nonkanker" labels
Step 5: Data Augmentation with ImageDataGenerator
Step 6: Building a CNN model
Step 7: Training the model
Step 8: Model evaluation
Step 9: Save the model in a pickle format file
Step 10: Embedding models into web-based applications
Step 11: Web-based cancer and non-cancer image prediction testing

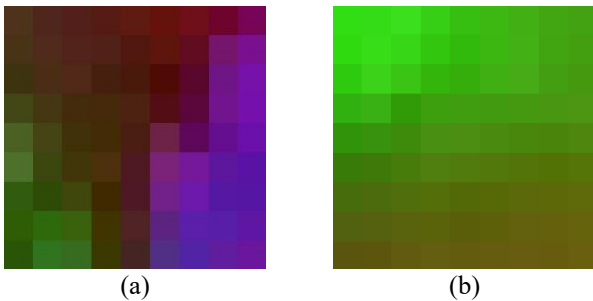


Figure 2. Sample of a 9-pixel patch from an image labeled as (a) “Kanker” and (b) “Nonkanker”

This color conversion process also ensures that variations in lighting conditions do not adversely affect the output, as the HSV color space is designed to separate color information (hue and saturation) from brightness (value). By isolating the hue and saturation components, which are less sensitive to changes in illumination, the preprocessing step minimizes the impact of different lighting conditions commonly found in smartphone-captured images. As a result, the model can consistently detect and interpret the visual patterns related to cancerous and non-cancerous tissues, even under varying lighting environments. This approach enhances the reliability of feature extraction, allowing for more robust classification in the subsequent analysis stages.

The dataset used in this study consists of 138 images acquired through a standard camera labeled “kanker” and “nonkanker” images. 112 images (80%) were allocated for model training, while the remaining 26 images (20%) were used for testing, as shown in Figure 3. Variations in the dataset posed a significant challenge to the model, mainly due to differences in image quality, lighting, and image capture position. Therefore, a comprehensive preprocessing strategy is required to ensure that the input data is standardized as much as possible before training the CNN model. The labeling process was performed manually to ensure accuracy, and the clustering results showed the dataset was ready for the training and evaluation stages of the model.

Data augmentation was done to increase the number and variety of training datasets using the ImageDataGenerator function. Augmentation techniques include rescaling to normalize pixel values to a scale of 0 to 1, shear transformation with a range of 0.2, zooming with a range of 0.2, and horizontal flipping. Later, the photos were reduced to 150x150 pixels and batched into 32 images to speed up the model training process. The augmentation boosted the dataset's visual diversity, allowing the model to learn more complicated patterns and prepare for more accurate model validation.

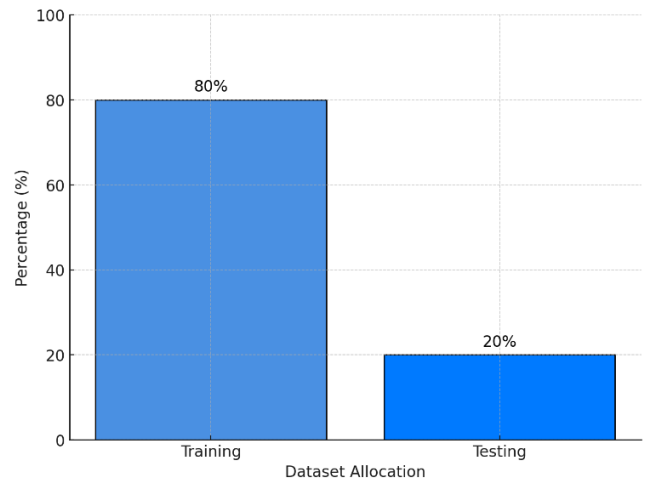


Figure 3. Distribution of datasets for model training and testing

The hyperparameter values utilized during model training are given below to provide additional insight into training and validation results. The input image size was standardized to 150x150 pixels, and a batch size 32 was used for training and validation data. To increase the training dataset's diversity, data augmentation techniques such as normalization (rescaling pixel values to [0, 1]), shear transformations (shear range: 0.2), zoom augmentation (zoom range: 0.2), and horizontal flipping were used. The Convolutional Neural Network (CNN) architecture consisted of three convolutional layers with progressively increasing filters (32, 64, and 128), each followed by MaxPooling2D layers with a pool size 2x2. A dense layer with 128 units, ReLU activation, and a dropout rate 0.5 was used to mitigate overfitting. The model was compiled with the Adam optimizer (learning rate: 0.001, default parameters) and binary cross entropy loss function, and accuracy was employed as the evaluation metric.

Figure 4 shows the performance of models trained with and without data augmentation over multiple epochs. The model with augmentation (orange line) exhibits a rapid increase in accuracy, peaking at approximately 0.80 in the third epoch, followed by fluctuations. Despite the fluctuations, the accuracy improves significantly towards the end, reaching the highest point at around 0.85. In contrast, the model without augmentation (blue line) demonstrates a slower but more stable improvement, with accuracy reaching approximately 0.70 by the fifth epoch and remaining consistent afterward. This suggests that data augmentation helps the model achieve higher peak accuracy and better generalization, although it introduces some instability during training. The model without augmentation is more stable but does not reach the same level of accuracy as the augmented model. Based on these findings, subsequent processes will utilize the augmented data to

optimize model performance.

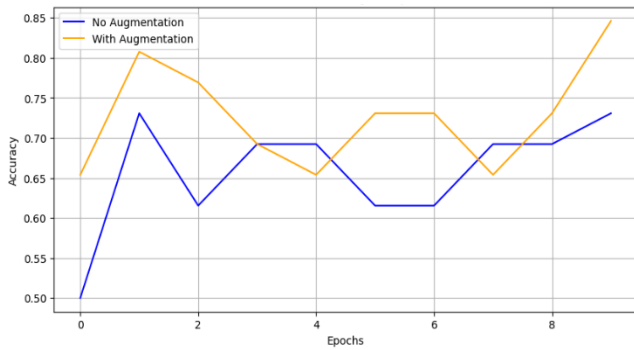


Figure 4. Validation accuracy comparison

The model was trained for 10 epochs, with the steps per epoch and validation steps calculated based on the batch and dataset sizes. While the training accuracy steadily increased during the initial epochs, the observed training and validation accuracy fluctuations, as depicted in Figure 5, suggest a potential limitation in the model's ability to generalize to unseen data. This behavior highlights the impact of hyperparameter settings, such as the relatively small number of epochs and the use of data augmentation, on the training process. Addressing these restrictions, such as fine-tuning the dropout rate or additional regularization approaches, may increase the model's generalizability.

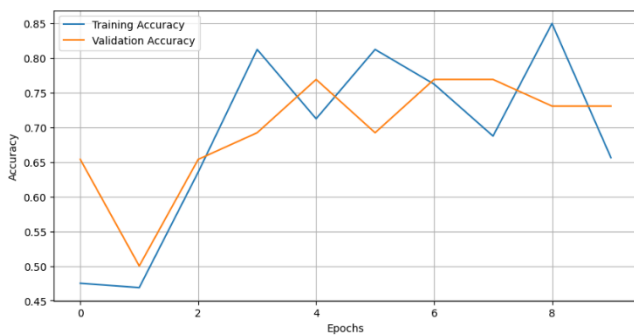


Figure 5. Training and validation accuracy

Figure 6 shows the training and validation loss graph for 10 epochs of model training. The overall loss of the training data decreases from the initial epoch, with a significant downward trend until around the 4th epoch, although there are minor fluctuations in subsequent epochs. In contrast, the loss on the validation data experienced larger fluctuations, with significant increases in some epochs, such as the 6th epoch, before decreasing again in subsequent epochs. This pattern suggests that while the model can reduce the loss on training data, its performance on validation data is not yet fully stable. It may face difficulties in generalizing patterns from training data to validation data. Fluctuations in validation loss could also be a sign of overfitting or imbalance in the validation data.

Performance by the model is represented in the confusion matrix, shown in Figure 7, through a comprehensive view of the classification outcomes: true positives (TP), true negatives (TN), false positives (FP), and false negatives (FN). The model correctly identified several true positive cases; that is, cancer images correctly classified as "kanker." These results are vital to support early detection and treatment of breast cancer. Besides, many true negatives were also successful; that

is, non-cancerous images were correctly classified as "nonkanker", which underlines the capability of the model to correctly recognize healthy breast tissue without raising superfluous alarms.

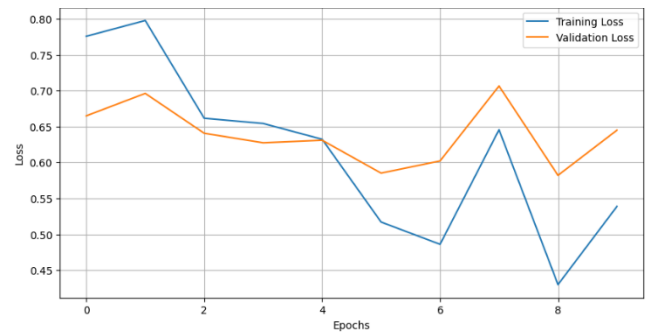


Figure 6. Training and validation loss

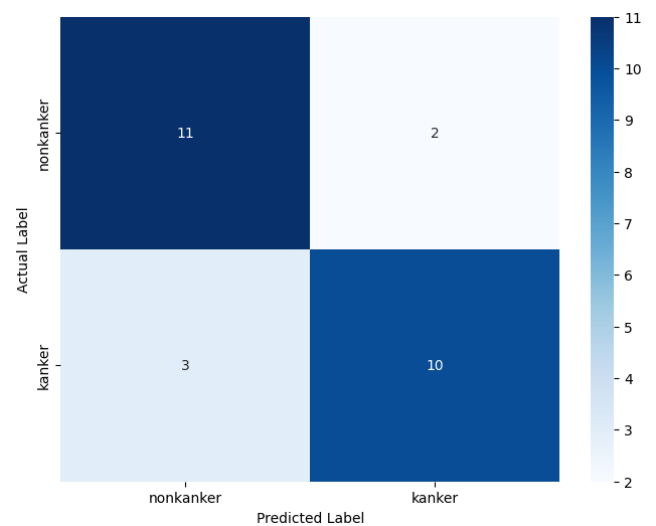


Figure 7. CNN confusion matrix

However, there are some misclassifications in the model. False positives, where non-cancerous images are incorrectly classified as "kanker," may lead to unnecessary follow-up tests and increased emotional distress for patients. These inaccuracies can be ascribed to the extensive area captured in certain photos, where the patient's attire is visible, generating noise miming malignant characteristics. Conversely, instances of false negatives, in which malignant pictures are erroneously categorized as "nonkanker," are of considerable concern. Minor tumors next to the areola may be erroneously identified as the areola, resulting in misdiagnosis. The inability to identify cancer may postpone essential treatment, potentially leading to severe health repercussions. These challenges underscore the necessity of standardizing image acquisition to concentrate on the pertinent area and employing accurate segmentation techniques to minimize noise. Achieving an equilibrium between false positives and negatives is essential for optimizing the model's efficacy and improving its practical applicability in clinical settings.

The ROC curve in Figure 8 illustrates the model's performance in distinguishing between cancer and noncancer cases. The curve is plotted using the True Positive Rate (TPR) against the False Positive Rate (FPR) at various threshold levels. The Area Under the Curve (AUC) is estimated as 0.71, showing that the model can moderately differentiate between

the two classes. The ROC curve provides insight into the trade-off between sensitivity (recall) and specificity, showing that the model can identify patterns associated with cancerous and non-cancerous images. However, further optimization may improve its discriminative performance.

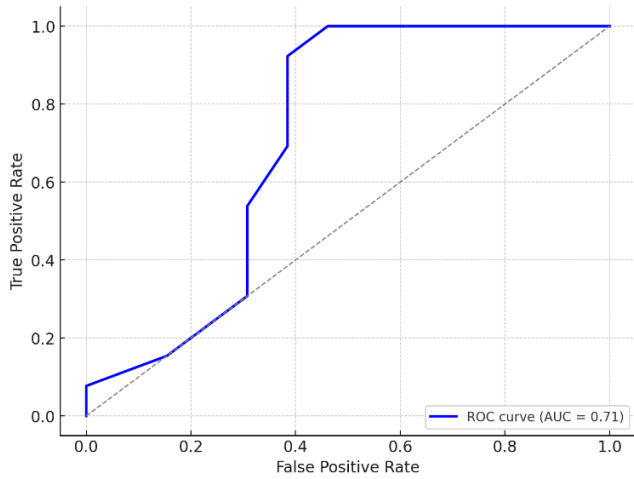


Figure 8. Receiver Operating Characteristic (ROC) curve

Table 1. CNN performance metrics

Class	Precision	Recall	F1-Score	Support
Kanker	79%	85%	81%	13
Nonkanker	83%	77%	80%	13
MacroAvg	81%	81%	81%	26
WeightedAvg	81%	81%	81%	26
Accuracy			81%	26

Table 1 shows the model's performance metrics for each class. The model achieved an accuracy of 81%, which demonstrates its effectiveness in classifying cancer and non-cancer images. Interestingly, the macro average and weighted average values for precision, recall, and F1-score are all the same at 81%. The precision of 79% for “kanker” and 83% for “nonkanker” shows that the model can reduce the number of false positives, thus providing more accurate diagnosis detection. A recall of 81% indicates the model's good sensitivity in identifying cancer patients, reducing the potential for missed diagnoses. The F1-score value of 81% reflects a balanced combination of precision and recall. In addition, the support metric shows that all validation datasets have been used and identified in this section. While these results are very optimistic, further research is needed to address the presence of false positives and false negatives.

Once training is complete, the model is saved in the pickle file format to ensure integration flexibility into various applications. The pickle format allows the storage of Python objects, including the model structure, weights, and parameters that have been trained, in the form of a file that can be easily reloaded without requiring retraining. These files are helpful for practical implementations, such as testing and deploying models on web application platforms. In web applications, pickle files allow saved models to be used in real-time in image classification without rebuilding or training the model from scratch. This process increases efficiency and makes testing models on various platforms easier, ensuring speed and accuracy in providing predictive results.

Figure 9 shows the directory structure of a Python-based application project using the Flask framework, where the trained model file, model.pkl, is embedded in the application to support the prediction process. The model.pkl file is stored in the models' folder, designed to store model-related files in an organized manner. The main script, app.py, loads the model from the folder, processes user requests, and generates predictions based on data uploaded through the web interface. The templates folder contains the index.html file as the user interface for uploading data and displaying prediction results. In contrast, the static folder stores static files, such as images or CSS, that support the application's appearance. This structure ensures efficient model integration and organized file management within the application.

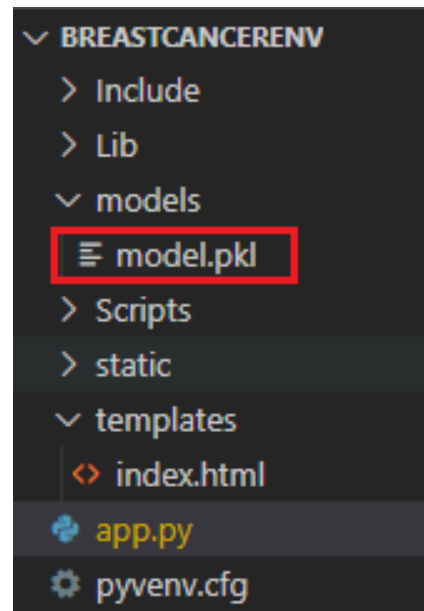


Figure 9. Model.pkl file in web application directory

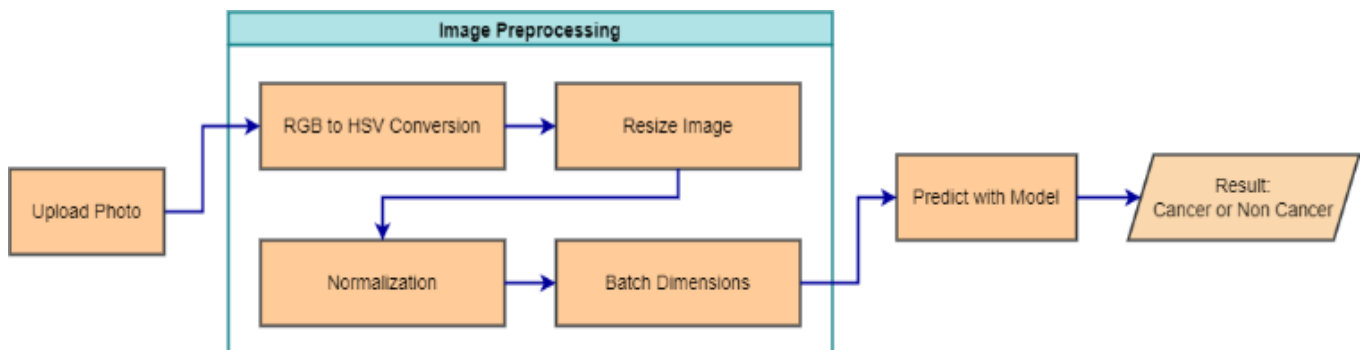


Figure 10. The schematic of the implementation process

The schematic of the implementation process, as shown in Figure 10, and the accompanying script outline a cancer detection system based on Flask. This web-based platform testing framework utilizes a pre-trained model stored in the model.pkl file to perform real-time predictions. The process begins when users upload an image, which undergoes preprocessing steps such as color space conversion (RGB-to-HSV), resizing to 150×150 pixels, pixel value normalization within the [0,1] range, and adding batch dimensions. Once preprocessed, the image is passed to the pre-trained model, which generates predictions based on extracted features. The results, identified as "Cancer" or "Non-Cancer," are shown alongside the uploaded image on the user interface, offering a smooth and intuitive experience for monitoring analysis outcomes.

Figure 11 illustrates that the model recognized the image as indicative of cancer, accomplishing this classification in a rapid 0.11 seconds using a central processing unit (CPU). The quick inference time underscores the effectiveness of the prediction process. This rapid inference time highlights the efficiency of the prediction process. Furthermore, the model has a total of 4,828,481 parameters, which underscores its architectural complexity. The rapid inference time highlights the model's ability to provide real-time or near-real-time predictions, rendering it appropriate for clinical applications. Further validation and optimization may be necessary to improve its reliability and generalization across various datasets.

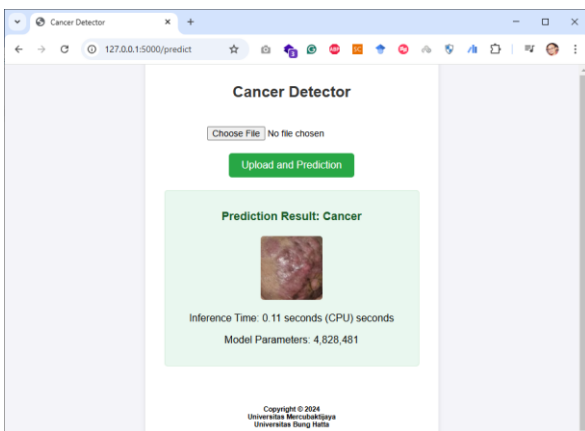


Figure 11. Prediction results: Cancer from user-uploaded images

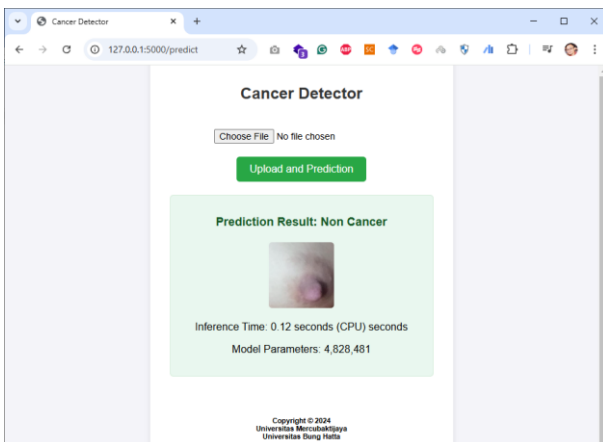


Figure 12. Prediction results: Noncancer from user-uploaded images

In Figure 12, the model classified the image as non-cancer with an inference time of 0.12 seconds (CPU), indicating efficient processing using the central processing unit. The model's complexity is reflected in its 4,828,481 parameters, suggesting a robust architecture. The quick inference time demonstrates the model's capability for real-time or near-real-time predictions, making it suitable for clinical applications. However, further validation and optimization may be required to enhance its reliability and generalization across diverse datasets.

3.2 Discussions

The examination of misclassifications identified two primary challenges. False positives frequently arose from artifacts, including shadows, skin folds, or reflections that mimicked cancerous tissue, highlighting the necessity for improved preprocessing to reduce these complications. False negatives were attributed to the model's challenges in identifying subtle tumors, as well as inconsistencies in breast positioning and lighting. This underscores the necessity for standardized imaging conditions to enhance reliability.

Conventional methods for breast cancer detection depend on high-quality histopathology [4, 30-37] or mammogram images [1, 29, 33, 38-41]. Access to methods processed through machine learning or manual analysis is frequently restricted in remote areas where hospitals are limited. The proposed model, which employs mobile phone images, achieved an accuracy of over 81%, demonstrating its potential as a feasible solution in resource-limited environments.

The performance has been negatively affected by inconsistent image quality, differing perspectives, and non-standard lighting conditions. While manual cropping and segmentation increase input refinement, this method is labor-intensive and does not ensure uniform quality across all photos. Future advancements may involve adopting automated preprocessing techniques, like adaptive histogram equalization and segmentation, to handle these concerns successfully.

In contrast to models that exploit mammographic or ultrasound images [1, 42] known for obtaining higher accuracy due to superior input quality—this proposed method remains adaptive and practical despite working with lower-quality inputs. This adaptability underlines the possibility for continued evolution, guaranteeing that the proposed method can efficiently handle diverse input quality requirements while giving dependable outcomes. A comparison with other comparable studies may be observed in Table 2.

While this study's accuracy correlates closely with past studies, it offers a more straightforward and more accessible approach. Utilizing only a cellphone camera, this method allows for immediate assessment of potential breast cancer detection. Results are presented through a web application, enabling patients and their families to receive timely information without needing hospital visits for early cancer screening. This innovation is particularly advantageous for individuals in remote areas, as it reduces the financial burden of traveling to urban centers for mammograms, which often entail longer waiting periods for results. In contrast, the findings from this study are available in just a few seconds.

To advance this study, future studies should focus on gathering more balanced and higher-quality datasets through collaborations with healthcare facilities. Combined with automated preprocessing and transfer learning, these

initiatives could considerably increase the system's accuracy and dependability. Despite its limitations, the model's success with cell phone photos shows its potential as a diagnostic support tool in settings with limited access to modern imaging equipment.

Since this study is still in its early stages, the dataset used

represents breast cancer cases in general without specific categorization based on tumor size. Future research will address this limitation by incorporating datasets categorized by tumor size, which is crucial for enhancing the model's clinical applicability and performance in detecting tumors of various dimensions.

Table 2. Comparison to related study

Topics	Input	Output	Testing Platform
Combining mammograms and health records to improve breast cancer detection accuracy [16]	Clinical health records, Mammography Images	84.5% accuracy	n.a.
Breast cancer detection using deep learning with CNNs for classifying cancerous cells [17]	Histopathological Images	82% accuracy	n.a.
Breast Cancer Detection Using Convolutional Neural Networks [18]	Mammography Images	84% accuracy	n.a.
Breast cancer image detection and classification using residual connected Convolutional Neural Networks (CNN) [19]	Histopathological Images	85.5% accuracy	n.a.
Proposed Method	Cellphone Camera Images	81% accuracy	Web app

False negatives still cause immense worry since they might postpone diagnosis and aggravate illnesses. Advanced cancer is more challenging to treat; consequently, early identification is vitally crucial. However, this strategy is aimed at first screening rather than a conclusive diagnosis. While tumor size will raise therapeutic relevance, advances in dataset quality, preprocessing, and transfer learning will improve performance. These actions will lower false negatives and increase the dependability of the model for practical usage.

4. CONCLUSIONS

This study developed and evaluated a Convolutional Neural Network (CNN) model for breast cancer detection using mobile phone images, achieving an accuracy of over 85% despite challenges related to image quality and dataset imbalance. The promising results demonstrate the model's potential for use in resource-limited environments, showcasing its effectiveness in classifying both “kanker” and “nonkanker” cases. However, improvements are needed, such as employing transfer learning with pre-trained models and obtaining a more extensive, balanced dataset, which could further boost performance. Overall, this system shows strong potential as a diagnostic support tool for early breast cancer detection, particularly in environments lacking access to high-quality imaging resources.

ACKNOWLEDGMENT

The authors would like to thank Direktur Riset, Teknologi, dan Pengabdian Kepada Masyarakat (DRTPM) of the Direktorat Jenderal Pendidikan Tinggi Kementerian Pendidikan dan Kebudayaan Republik Indonesia for research financial support under Fundamental Research - Regular with contract no. 112/E5/PG.02.00.PL/2024, and Lembaga Penelitian dan Pengabdian kepada Masyarakat (LPPM) Universitas Mercubaktijaya for publication support of 2024.

REFERENCES

[1] Qasim, K.R., Ouda, A.J. (2020). An accurate breast cancer detection system based on deep learning CNN. *Medico-Legal Update*, 20(1): 984-990.

<https://doi.org/10.37506/v20/i1/2020/mlu/194726>

[2] Zhou, X.J., Li, Y., Gururajan, R., Bargshady, G., Tao, X., Venkataraman, R., Kondalsamy-Chennakesavan, S. (2020). A new deep convolutional neural network model for automated breast cancer detection. In 2020 7th International Conference on Behavioural and Social Computing (BESC), Bournemouth, United Kingdom, pp. 1-4. <https://doi.org/10.1109/BESC51023.2020.9348322>

[3] Malve, P., Gulhane, V. (2024). Design of a multiple phased convolution model for pre-emption of breast cancer via extensive learning operations (MPC2EL). *Procedia Computer Science*, 233: 638-650. <https://doi.org/10.1016/j.procs.2024.03.253>

[4] Lu, S.Y., Wang, S.H., Zhang, Y.D. (2023). BCDNet: An optimized deep network for ultrasound breast cancer detection. *IRBM*, 44(4): 100774. <https://doi.org/10.1016/j.irbm.2023.100774>

[5] Wu, J.M., Tien, C.Y. (2023). Mobile-aided breast cancer diagnosis by deep convolutional neural networks. In *Research Anthology on Medical Informatics in Breast and Cervical Cancer*. PA: IGI Global, pp. 844-858. <https://doi.org/10.4018/978-1-6684-7136-4.ch044>

[6] Al Husaini, M.A.S., Hadi Habaebi, M., Gunawan, T.S., Islam, M.R. (2021). Self-detection of early breast cancer application with infrared camera and deep learning. *Electronics*, 10(20): 2538. <https://doi.org/10.3390/electronics10202538>

[7] Maistry, B., Ezugwu, A.E. (2023). Breast cancer detection and diagnosis: A comparative study of state-of-the-arts deep learning architectures. *arXiv preprint arXiv:2305.19937*. <https://doi.org/10.48550/arXiv.2305.19937>

[8] Rusydi, M.I., Amrina, E., Winata, Y., Nofendra, R. (2023). Threshold-based electroencephalography brain-computer interface for robot arm control. In 2023 8th Asia-Pacific Conference on Intelligent Robot Systems (ACIRS), Xi'an, China, pp. 113-117. <https://doi.org/10.1109/ACIRS58671.2023.10240250>

[9] Nakajima, R., Rusydi, M.I., Ramadhani, S.A., Muguro, J., Matsushita, K., Sasaki, M. (2022). Image presentation method for human machine interface using deep learning object recognition and P300 brain wave. *JOIV: International Journal on Informatics Visualization*, 6(3): 736-742. <https://doi.org/10.30630/joiv.6.3.949>

[10] Halake, D.G., Ogoncho, I.M. (2017). The role of mobile health in supporting cancer prevention, detection,

- treatment and palliative care in low and middle income countries: A scoping review. *Public Health Research*, 7(6): 123-135. <https://doi.org/10.5923/j.phr.20170706.01>
- [11] Rajakumari, R., Kalavani, L. (2022). Breast cancer detection and classification using deep CNN techniques. *Intelligent Automation & Soft Computing*, 32(2): 1089-1107. <https://doi.org/10.32604/iasc.2022.020178>
- [12] Ravnik, D., Jerman, T., Pernuš, F., Likar, B., Špiclin, Ž. (2018). Dataset variability leverages white-matter lesion segmentation performance with convolutional neural network. In *Medical Imaging 2018: Image Processing*, Houston, Texas, United States, pp. 388-396. <https://doi.org/10.1117/12.2293702>
- [13] Sharaf, A.I., Radwan, E.S.F. (2019). An automated approach for developing a convolutional neural network using a modified firefly algorithm for image classification. In *Applications of Firefly Algorithm and its Variants: Case Studies and New Developments*, Springer, Singapore, pp. 99-118. https://doi.org/10.1007/978-981-15-0306-1_5
- [14] Sai Krishna, N.M., Priyakanth, R., Katta, M.B., Akanksha, K., Anche, N.Y. (2023). CNN-based breast cancer detection. In *Proceedings of Fourth International Conference on Computer and Communication Technologies*, pp. 613-622. https://doi.org/10.1007/978-981-19-8563-8_59
- [15] Hamid, M.A., Mondher, H.M., Ayoub, B. (2024). Deep learning CNNs for breast cancer classification and detection” enhancing diagnostic accuracy in medical practice. In *2024 2nd International Conference on Electrical Engineering and Automatic Control (ICEEAC)*, Setif, Algeria, pp. 1-6. <https://doi.org/10.1109/ICEEAC61226.2024.10576560>
- [16] Trang, N.T.H., Long, K.Q., An, P.L., Dang, T.N. (2023). Development of an artificial intelligence-based breast cancer detection model by combining mammograms and medical health records. *Diagnostics*, 13(3): 346. <https://doi.org/10.3390/diagnostics13030346>
- [17] Gami, B., Chauhan, K., Panchal, B.Y. (2023). Breast cancer detection using deep learning. In *Mobile Radio Communications and 5G Networks*, Springer, pp. 85-95. https://doi.org/10.1007/978-981-19-7982-8_8
- [18] Hadush, S., Girmay, Y., Sinamo, A., Hagos, G. (2023). Breast cancer detection using convolutional neural networks. In *2022 International Symposium on Multidisciplinary Studies and Innovative Technologies (ISMSIT)*, 597-601. <https://doi.org/10.48550/arXiv.2003.07911>
- [19] Dai, C. (2024). Study on breast cancer image detection and classification based on residual connected convolutional neural network (CNN). *Theoretical and Natural Science*, 33(1): 224-230. <https://doi.org/10.54254/2753-8818/33/20240914>
- [20] Yadav, R., Maurya, S., Sharma, S., Gaurav, S., Agrawal, M. (2024). Breast cancer detection using CNN. *International Journal for Multidisciplinary Research*, 6(3): 1-11. <https://doi.org/10.36948/ijfmr.2024.v06i03.21254>
- [21] Zainudin, Z., Shamsuddin, S.M., Hasan, S. (2019). Deep learning layer convolutional neural network (CNN) scheme for cancer image. *IOP Conference Series: Materials Science and Engineering*, 551(1): 012039. <https://doi.org/10.1088/1757-899X/551/1/012039>
- [22] Sedigh, P., Sadeghian, R., Masouleh, M.T. (2019). Generating synthetic medical images by using GAN to improve CNN performance in skin cancer classification. In *2019 7th International Conference on Robotics and Mechatronics (ICRoM)*, Tehran, Iran, pp. 497-502. <https://doi.org/10.1109/ICRoM48714.2019.9071823>
- [23] Fitrilina, Rusydi, M.I., Kurnia, R., Sunaryo, B., Ramadhani, S.A. (2024). A systematic review of noninvasive blood glucose estimation using near infrared. *International Journal of Intelligent Systems and Applications in Engineering*, 12(4): 59-76.
- [24] Dafni Rose, J., VijayaKumar, K., Singh, L., Sharma, S.K. (2022). Computer-aided diagnosis for breast cancer detection and classification using optimal region growing segmentation with MobileNet model. *Concurrent Engineering*, 30(2): 181-189. <https://doi.org/10.1177/1063293X221080518>
- [25] Ferracuti, F., Iarlori, S., Mansour, Z., Monteriù, A., Porcaro, C. (2021). Comparing between different sets of preprocessing, classifiers, and channels selection techniques to optimise motor imagery pattern classification system from EEG pattern recognition. *Brain Sciences*, 12(1): 57. <https://doi.org/10.3390/brainsci12010057>
- [26] Chicco, D., Tötsch, N., Jurman, G. (2021). The Matthews correlation coefficient (MCC) is more reliable than balanced accuracy, bookmaker informedness, and markedness in two-class confusion matrix evaluation. *BioData Mining*, 14: 13. <https://doi.org/10.1186/s13040-021-00244-z>
- [27] Úbeda, A., Azorín, J.M., Farina, D., Sartori, M. (2018). Estimation of neuromuscular primitives from EEG slow cortical potentials in incomplete spinal cord injury individuals for a new class of brain-machine interfaces. *Frontiers in Computational Neuroscience*, 12: 3. <https://doi.org/10.3389/fncom.2018.00003>
- [28] Fernández-Rodríguez, Á., Velasco-Álvarez, F., Bonnet-Save, M., Ron-Angevin, R. (2018). Evaluation of switch and continuous navigation paradigms to command a brain-controlled wheelchair. *Frontiers in Neuroscience*, 12: 438. <https://doi.org/10.3389/fnins.2018.00438>
- [29] Elaraby, A., Saad, A., Elmannai, H., Alabdulhafith, M., Hadjouni, M., Hamdi, M. (2024). An approach for classification of breast cancer using lightweight deep convolution neural network. *Heliyon*, 10(20): e38524, 2024, <https://doi.org/10.1016/j.heliyon.2024.e38524>
- [30] Ge, R., Chen, G., Saruta, K., Terata, Y. (2024). Detection of presence or absence of metastasis in WSI patches of breast cancer using the dual-enhanced convolutional ensemble neural network. *Machine Learning with Applications*, 17: 100579. <https://doi.org/10.1016/j.mlwa.2024.100579>
- [31] Kaul, N., Zaman, M., Bakshi, W.J., Kaul, S., Bhat, B., Fayaz, S.A. (2024). Analytical study of breast cancer and treatment techniques. *Procedia Computer Science*, 235: 578-587. <https://doi.org/10.1016/j.procs.2024.04.057>
- [32] Qi, Y.J., Su, G.H., You, C., Zhang, X., Xiao, Y., Jiang, Y.Z., Shao, Z.M. (2024). Radiomics in breast cancer: Current advances and future directions. *Cell Reports Medicine*, 5(9): 101719. <https://doi.org/10.1016/j.xcrm.2024.101719>
- [33] Desai, M., Shah, M. (2021). An anatomization on breast cancer detection and diagnosis employing multi-layer perceptron neural network (MLP) and convolutional

- neural network (CNN). *Clinical eHealth*, 4: 1-11. <https://doi.org/10.1016/j.ceh.2020.11.002>
- [34] Yu, D., Lin, J., Cao, T., Chen, Y., Li, M., Zhang, X. (2023). SECS: An effective CNN joint construction strategy for breast cancer histopathological image classification. *Journal of King Saud University-Computer and Information Sciences*, 35(2): 810-820. <https://doi.org/10.1016/j.jksuci.2023.01.017>
- [35] Gupta, K., Chawla, N. (2020). Analysis of histopathological images for prediction of breast cancer using traditional classifiers with pre-trained CNN. *Procedia Computer Science*, 167: 878-889. <https://doi.org/10.1016/j.procs.2020.03.427>
- [36] Solorzano, L., Robertson, S., Acs, B., Hartman, J., Rantalainen, M. (2024). Ensemble-based deep learning improves detection of invasive breast cancer in routine histopathology images. *Heliyon*, 10(12): e32892. <https://doi.org/10.1016/j.heliyon.2024.e32892>
- [37] Krishna, S., Suganthi, S.S., Bhavsar, A., Yesodharan, J., Krishnamoorthy, S. (2023). An interpretable decision-support model for breast cancer diagnosis using histopathology images. *Journal of Pathology Informatics*, 14: 100319. <https://doi.org/10.1016/j.jpi.2023.100319>
- [38] Sereshkeh, E.T., Keivan, H., Shirbandi, K., Khaleghi, F., Asl, M.M.B. (2024). A convolution neural network for rapid and accurate staging of breast cancer based on mammography. *Informatics in Medicine Unlocked*, 47: 101497. <https://doi.org/10.1016/j.imu.2024.101497>
- [39] Mendes, J., Oliveira, B., Araújo, C., Galvão, J., Garcia, N.C., Matela, N. (2024). Artificial intelligence on breast cancer risk prediction. *Societal Impacts*, 4: 100068. <https://doi.org/10.1016/j.socimp.2024.100068>
- [40] Alam, M.N.A., Uddin, K.M.M., Rahman, M.M., Manu, M.M.R., Nasir, M.K. (2024). A novel automated system to detect breast cancer from ultrasound images using deep fused features with super resolution. *Intelligence-Based Medicine*, 10: 100149. <https://doi.org/10.1016/j.ibmed.2024.100149>
- [41] Hossain, S., Azam, S., Montaha, S., Karim, A., Chowa, S.S., Mondol, C., Jonkman, M. (2023). Automated breast tumor ultrasound image segmentation with hybrid UNet and classification using fine-tuned CNN model. *Heliyon*, 9(11): e21369. <https://doi.org/10.1016/j.heliyon.2023.e21369>
- [42] Alotaibi, M., Aljouie, A., Alluhaidan, N., Qureshi, W., Almatar, H., Alduhayan, R., Almazroa, A. (2023). Breast cancer classification based on convolutional neural network and image fusion approaches using ultrasound images. *Heliyon*, 9(11): e22406. <https://doi.org/10.1016/j.heliyon.2023.e22406>